Published in final edited form as:
Dev Biol. 2008 February 1; 314(1): 137–149. doi:10.1016/j.ydbio.2007.11.022.

Drosophila ELMO/CED-12 interacts with Myoblast city to direct myoblast fusion and ommatidial organization

Erika R. Geisbrecht[1], **Shruti Haralalka**[1], **Selene K. Swanson**[2], **Laurence Florens**[2], **Mike P. Washburn**[2], and **Susan M. Abmayr**[1]

1 *Stowers Institute for Medical Research, 1000 E. 50th St, Kansas City, MO 64110 USA*

2 *Proteomics core facility, Stowers Institute for Medical Research, 1000 E. 50th St, Kansas City, MO 64110 USA*

Abstract

Members of the CDM (CED-5, Dock180, Myoblast city) superfamily of guanine nucleotide exchange factors function in diverse processes that include cell migration and myoblast fusion. Previous studies have shown that the SH3, DHR1 and DHR2 domains of Myoblast city (MBC) are essential for it to direct myoblast fusion in the *Drosophila* embryo, while the conserved DCrk-binding proline rich region is expendable. Herein, we describe the isolation of *Drosophila* ELMO/CED-12, an ~82 kD protein with a pleckstrin homology (PH) and proline-rich domain, by interaction with the MBC SH3 domain. Mass spectrometry confirms the presence of an MBC/ELMO complex within the embryonic musculature at the time of myoblast fusion and embryos maternally and/or zygotically mutant for *elmo* exhibit defects in myoblast fusion. Overexpression of MBC and ELMO in the embryonic mesoderm causes defects in myoblast fusion reminiscent of those seen with constitutively-activated Rac1, supporting the previous finding that both the absence of and an excess of Rac activity are deleterious to myoblast fusion. Overexpression of MBC and ELMO/CED-12 in the eye causes perturbations in ommatidial organization that are suppressed by mutations in *Rac1* and *Rac2*, demonstrating genetically that MBC and ELMO/CED-12 cooperate to activate these small GTPases in *Drosophila*.

Keywords

Drosophila; ELMO; MBC; Rac; myoblast fusion; ommatidial organization

INTRODUCTION

Drosophila myoblast city (MBC), *C. elegans* CED-5, and vertebrate DOCK180, are closely related members of the evolutionarily conserved CDM family of proteins (Erickson et al., 1997; Hasegawa et al., 1996; Wu and Horvitz, 1998b). They serve as key players in a signaling complex that includes the SH2-SH3 domain-containing adaptor protein CrkII/CED-2 and the PH domain containing protein ELMO/CED-12 (reviewed in (Meller et al., 2005)). This complex then acts at the membrane to relay signals to the small GTPase Rac1/CED-10. MBC/

Address All Correspondence to Susan M. Abmayr, Ph.D. (E-mail: sma@stowers-institute.org)., Phone: 816-926-4393, Fax: 816-926-4693.

DOCK180/CED-5 function as non-conventional Guanine nucleotide Exchange Factors (GEFs) for Rac. Conventional GEFs bind to nucleotide-free Rac via a Dbl-homology (DH) domain, thereby facilitating exchange of GDP for GTP. DOCK180/CED-5, which lack DH domains, associate with nucleotide-free Rac through a conserved Dock-Homology Region (DHR2) (Brugnera et al., 2002; Cote and Vuori, 2002). Deletion of this domain results in loss of Rac binding and the inability to direct formation of GTP-bound Rac (Brugnera et al., 2002).

In addition to DHR2, CDM proteins have in common an N-terminal SH3 domain, a second Dock Homology Region (DHR1), and a C-terminal proline rich region. The C-terminal region directs interaction with the SH3 domain of CrkII/CED-2. The CrkII SH2 domain can then direct interaction with upstream proteins that are phosphorylated on tyrosine, such as transmembrane receptors and components of focal adhesions (Cheresh et al., 1999; Kiyokawa et al., 1998). In addition to membrane recruitment through Crk-related interactions, the C-terminal PH domain of ELMO/CED-12 can also mediate its membrane localization (deBakker et al., 2004; Grimsley et al., 2004). The DHR1 region of DOCK180, which binds to phosphatidylinositol 3,4,5-triphosphate [PtdIns(3,4,5)P_3], is also required for its membrane localization (Cote et al., 2005; Kobayashi et al., 2001). The N-terminal SH3 domains of DOCK180 and CED-5 mediate interaction with the C-terminal proline-rich region of ELMO and CED-12, respectively (Lu et al., 2004; Lu et al., 2005; Wu et al., 2001). *In vitro* studies demonstrate that DOCK180 binding to Rac can be sufficient for its activation (Cote et al., 2005), but that this activation can be significantly enhanced by DOCK180 bound to ELMO (Brugnera et al., 2002; Katoh and Negishi, 2003; Lu et al., 2004). Thus, the DOCK180/ELMO complex is a key component in CDM signaling to Rac.

In addition to extensive homology and conserved biochemical interactions between the DOCK180/CED-5 and ELMO/CED-12 protein families, complexes of these proteins perform similar biological functions. For example, genetic studies have shown that *C. elegans* CED-10 acts with CED-2/Crk, CED-5/DOCK180 and CED-12/ELMO to promote cell migration of the distal tip cells during development of the somatic gonad and engulfment of cell corpses following apoptosis (Gumienny et al., 2001; Kinchen et al., 2005; Wu and Horvitz, 1998a; Zhou et al., 2001). Membrane targeted Dock180 increases cell spreading, and overexpression of wild-type Dock180 in mammalian cells enhances cell migration and phagocytosis of apoptotic cells (Cheresh et al., 1999; Kiyokawa et al., 1998). Lastly, a reduction in wild-type Dock180 or overexpression of mutant forms of DOCK180 decrease activated Rac and cause defects in cell spreading and cell migration (Cote and Vuori, 2002; Katoh and Negishi, 2003; Kiyokawa et al., 1998).

As in *C. elegans* and vertebrates, *Drosophila* MBC interacts genetically with other molecules required for CDM pathway function. For example, mutations in *mbc* delay border cell migration and influence PVR mediated F-actin accumulation in the follicle cells during ovary development, reflecting its proposed role in the PVR-Rac pathway (Duchek et al., 2001). Studies utilizing RNAi constructs have demonstrated a genetic interaction between MBC, *Drosophila* Crk (DCrk) and ELMO in adult thorax closure (Ishimaru et al., 2004). In the *Drosophila* eye, in which Rac is required for proper actin organization (Chang and Ready, 2000), the effects of Rac1 overexpression are suppressed by loss of one copy of *mbc* (Nolan et al., 1998). Rac1 was initially implicated in myoblast fusion in the embryo by the demonstration that overexpression of either dominant-negative or constitutively-active Rac1 interferes with myoblast fusion (Luo et al., 1994). More recently, loss-of-function studies have established that Rac1 and Rac2 play a redundant but essential role in this process. MBC is absolutely essential for myoblast fusion (Hakeda-Suzuki et al., 2002), where it colocalizes in founder myoblasts with the immunoglobulin superfamily member Duf/Kirre (Chen and Olson, 2001). MBC is also expressed in, and apparently required in, the fusion competent myoblasts (Balagopalan et al., 2006). Structure/function analysis of MBC identified the protein domains

that are essential for myoblast fusion. This analysis revealed that, like Dock180, the DHR1 domain binds to PtdIns(3,4,5)P_3 and is essential for myoblast fusion. The N-terminal SH3 domain and the putative Rac binding DHR2 domain are essential for MBC transgenes to rescue the myoblast fusion defects in *mbc* mutant embryos. Surprisingly, however, while the C-terminal proline-rich region directs a strong interaction with DCrk (Balagopalan et al., 2006; Ishimaru et al., 2004), this region is not required for MBC function in the embryonic musculature(Balagopalan et al., 2006). Thus, the canonical Crk-associated CDM pathway that has been described for other organisms and used in other *Drosophila* tissues (Bourne, 2005; Ishimaru et al., 2004; Reif and Cyster, 2002) does not appear to be used in *Drosophila* myoblast fusion. This finding raised the broader question of whether other components of the canonical pathway functioned along with MBC in the embryonic muscle, or whether MBC functions in this tissue through different protein interactions.

To address the involvement of *Drosophila* ELMO in signaling from MBC, we have isolated and characterized its role in myoblast fusion, border cell migration and ommatidial organization. Herein we demonstrate that ELMO is expressed in the ovary, where it interacts genetically with MBC and plays a role in border cell migration. We generate and analyze multiple loss-of-function alleles to demonstrate the importance of maternal and zygotic ELMO in myoblast fusion. We confirm, through a targeted mass spectrometry approach, that these proteins form a stable complex in the embryonic musculature. We demonstrate that ELMO and MBC act cooperatively in the mesoderm, such that an excess of both causes serious defects in myoblast fusion reminiscent of those seen with excess Rac activity. Finally, we establish genetically that ELMO and MBC can cooperate to activate Rac GTPases in the adult eye.

MATERIALS AND METHODS

Drosophila stocks

Fly stocks were raised on standard cornmeal medium at 25°C unless otherwise indicated. Oregon R was used as the wild-type strain. Fly stocks that were obtained from the Bloomington Stock Center include *UAS-mCD8-GFP, c306-GAL4, UAS-RacN17, PBac[c06760]/CyO, and Df(2L)Prl/CyO*. The *UAS-elmoIR, UAS-mbcIR* and *UAS-DCrkIR* transgenic lines were obtained from Ryu Ueda (Ishimaru et al., 2004). *UAS-elmo* and *UAS-elmoHA* were generated by standard methods and injected by Genetic Services, Inc. *UAS-mbc* and *UAS-mbcHA* have been described (Balagopalan et al., 2006). For analysis of the border cell migration phenotype, *slbo-Gal4; UAS-mCD8-GFP* or *c306-Gal4* flies were crossed to UAS transgenic flies. Non balancer progeny were fattened overnight at 29°C before dissection.

Molecular cloning of *elmo*

A full length cDNA of the *elmo* transcript was obtained by RT-PCR from Oregon R flies using standard methods with the forward primer GCGCCCGGGAATGATACCAAAAAAGACGACGG and the reverse primer CGCGCTCGAGTTAGCTCTCAAAGCAAAAATCATAG. The resulting PCR product was digested and cloned into the yeast 2-hybrid prey vector pGADT7 (Clontech). Full length *elmo* was amplified by PCR and cloned into pUAST using the forward primer ATAAGAATGCGGCCGCAATGATACCAAAAAAGACGACGG and the reverse primer GCTCTAGAGTTAGCTCTCAAAGCAAAAATC. For the HA-tagged *UAS-elmo* construct, sequences encoding the HA epitope were added to the 3′ end. All clones were verified by sequencing.

In situ hybridization and immunohistochemistry

Embryos were collected on agar-apple juice plates and aged at 25°C. For *in situ* analysis, full-length *elmo* was transcribed with Sp6 using the DIG mRNA labeling kit (Roche) and hybridized

as described (Tautz and Pfeifle, 1989). Myosin heavy chain was detected colorimetrically as described (Erickson et al., 1997)

Ovary dissections and immunofluorescence staining were performed as in Geisbrecht *et al.* (Geisbrecht and Montell, 2004). Antisera to ELMO was generated in rabbit using full length protein overexpressed in bacteria and used at 1:10. It was detected fluorescently using Alexa Fluor® 488 goat anti-rabbit IgG at 1:400 (Molecular Probes, Carlsbad, CA). 0.5 mg/ml DAPI (Sigma, Dallas, TX) and Alexa Fluor® 546-phalloidin at 1:400 (Molecular Probes, Carlsbad, CA) were added with the secondary antibodies.

Yeast 2-hybrid assays

The yeast 2-hybrid screen was performed by PanBionet Inc. Full length *elmo* cDNA was cloned as above and yeast 2-hybrid experiments to confirm this interaction were performed as in Balagopalan, *et al*. (Balagopalan et al., 2006).

Mass spectrometry

For both MBC and ELMO, HA-tagged and untagged transgenic flies were crossed to *mef2-GAL4* females and 6–18h embryos were collected on agar-apple juice plates at 25°C. For each immunopreicitation experiment, ~300 mg embryos were dechorionated and homogenized in lysis buffer [60mM Tris (pH 7.5), 80mM NaCl, 6mM EDTA (pH 8.0), 2% Triton X-100, 1mM Na_3VO_4, 5mM 1-Naphthyl phosphate potassium salt, 2mM PMSF, 2 ug/ml Leupeptin, 2 ug/ml Pepstatin]. The NaCl concentration was increased to 300mM and resulting lysate mixed with anti-HA resin overnight at 4°C. The resin was washed 3 times with wash buffer [60mM Tris (pH 7.5), 300mM NaCl, 6mM EDTA (pH 8.0), 1.0% Triton X-100] with protease inhibitors. Protein was eluted from the resin using 0.2 mg/ml 2x HA peptide. Samples were TCA-precipitated and digested as described (Florens and Washburn, 2006). Peptide digests were separated on 3-phase (reverse-phase/strong cation exchange/reverse phase) chromatography microcapillary columns(McDonald et al., 2002), and analyzed by Multidimensional Protein Identification Technology (MudPIT) (Washburn et al., 2001). Tandem mass (MS/MS) spectra were matched using SEQUEST (Eng et al., 1994) to peptides from a database of 35050 amino acid sequences, consisting of 17348 *D. melanogaster* proteins (non-redundant entries from NCBI 2006-11-28 release) and, to estimate false discovery rates, 17525 randomized sequences for each non-redundant protein entry. Peptide/spectrum matches were selected and compared using DTASelect/CONTRAST (Tabb et al., 2002) and were retained if they had a DeltCn of at least 0.08. Peptides had to be at least 7 amino acids long and their termini had to comply with the proteolytic enzyme selectivities. For trypsin digests, minimum cross-correlation scores (Xcorr) were set at 1.8 for singly-, 2.0 for doubly-, and 3.0 for triply-charged spectra, while for elastase digests, minimum XCorr were 2.5 for doubly-, and 3.5 for triply-charged spectra. Combining all runs, proteins had to be detected by at least 2 such peptides, or 1 peptide with 2 independent spectra. To estimate relative protein levels, Normalized Spectral Abundance Factors (NSAFs) were calculated for each non-redundant protein, as described in (Paoletti et al., 2006; Zybailov et al., 2006)

Generation and molecular characterization of *elmo* alleles

Isogenized $b^1 elA^1 rd^s pr^1\ cn^1 or^{49h}$ (Bloomington Stock Center) males were treated with 25mM EMS in 5% sucrose for 18–24h using standard methods, and the mutagenized males mated with *Gla/CyO, GAL4-twi, P{UAS-2xEGFP]* virgin females. Approximately 5000 CyO-balanced male progeny were mated individually to *PBac[c06760]/CyO* females. Stable stocks were generated from crosses that failed to complement, and balanced with *Gla/CyO, GAL4-twi, P{UAS-2xEGFP]*. For each EMS allele, the *elmo* genomic region was amplified by PCR from heterozygous flies using *elmo*-specific primers and the PCR products sequenced to identify the molecular lesion. All mutations were confirmed in multiple sequencing reactions

from independently amplified DNA samples. For RT-PCR, RNA from appropriately staged material was made using Trizol and subsequent RT-PCR was performed using *elmo*-specific primers by standard methods. *Df(2L)HO55* was made by P-element excision of the Bloomington stock 10539 in the downstream gene *aats-thr*. Removal of *elmo* was confirmed by PCR.

Generation of germ line and mosaic clones and RNAi analysis

The *elmo^{PB}*, *elmo^{8C6}*, *and elmo^{19F3}* mutations were recombined onto the FLP recombination target (FRT)-containing second chromosome of *w; al^{1} dp ov^{1} b^{1} pr^{1} P{ry[+t7.2]=neoFRT}40A* (Bloomington Stock Center) and mated to males of the genotype *hs-FLP22; P{ry[+t7.2]=neoFRT}40A, P{ovo^{D1}}/CyO*. Progeny from this cross were heat shocked at 37°C for 2h on days 4 and day 5 (late L2 or L3) as described (Balagopalan et al., 2006). Female progeny of the genotype *hs-FLP22/+; P{ry[+t7.2]=neoFRT}40A, P{ovo^{D1}}/P{ry[+t7.2]=neoFRT}40A, elmo** were recovered and crossed to *Df(2L)Prl/CyO, GAL4-twi, P{UAS-2xEGFP]* heterozygous males. The muscle pattern of embryos laid by these females was then examined as described above. For mosaic clonal analysis, larvae of the genotype *hs-FLP22/+; P{ry[+t7.2]=neoFRT}40A, P{ovo^{D1}}/P{ry[+t7.2]=neoFRT}40A, elmo^{19F3}, ubiGFP* were heat shocked as described (Niewiadomska et al., 1999). The ovaries of female progeny of the appropriate genotype were then dissected and examined as described above. For RNAi analysis in embryos, the progeny of *mef2-GAL4* or *mef2-GAL4/2x UAS-elmoIR* were grown at, 29°C until stage 16, immunostained with MHC as above, and unfused myoblasts were counted in hemisegments A2-A5.

Scanning Electron Microscope (SEM) analysis

Scanning electron micrographs of the eyes of adult flies of the correct genotype were taken using the Hitachi Tabletop Microscope TM-1000 according to manufacturer's suggestions.

RESULTS

Identification of ELMO as a binding partner for MBC in the *Drosophila* musculature

The SH3 domain of MBC is required during *Drosophila* muscle development (Balagopalan et al., 2006). We therefore used this domain as bait in a yeast two-hybrid screen of a *Drosophila* embryonic cDNA library to identify binding partners that may function with MBC in myoblast fusion. This screen resulted in the identification of CG5336, the *Drosophila* ortholog of ELMO/CED-12. The interaction between full length MBC, or MBC that lacks all proline rich regions, and full length ELMO was confirmed in a yeast two-hybrid assay (Fig. 1A). It was also confirmed by immunoprecipitation of lysate from S2 cells co-transfected with full length HA-tagged MBC and Flag-tagged ELMO in an analysis similar to that of Ishimaru *et al*. (Ishimaru et al., 2004)(data not shown).

In previous studies, similar assays had revealed a robust interaction between MBC and DCrk that is not required for MBC-mediated signaling in myoblast fusion (Balagopalan et al., 2006). Thus, as a first step in determining the relevance of the above MBC/ELMO complex to the embryonic musculature, we chose to use a proteomics analysis of MBC interactions in this tissue. Flies transgenic for either HA-tagged or untagged MBC under UAS control were crossed to flies bearing the muscle-specific *mef2-GAL4* driver, and lysates prepared from the resulting embryos at approximately 6–18 h AEL. Both transgenes are functional and rescue the myoblast fusion phenotype when expressed in the mesoderm of *mbc* mutant embryos (Balagopalan et al., 2006). HA-tagged MBC and associated proteins were then immunoprecipitated with anti-HA resin, and proteins in the immunoprecipitate analyzed in a silver stained gel, by western blot and by Multidimensional Protein Identification Technology

(MudPIT) mass spectrometry (Washburn et al., 2001). In control samples, lysate from untagged MBC was subjected to identical immunoprecipitation and analysis.

As shown in Figure 1B, a band corresponding to the expected molecular weight of ELMO was detected in a silver stained gel of total protein immunoprecipitated from lysates containing HA-tagged MBC but not untagged MBC. Immunobloting confirmed this result, detecting a strong band in the immunoprecipitate from HA-tagged MBC. A small amount of ELMO was also present in the control immunoprecipitate, and appeared to be due to nonspecific sticking of MBC to the HA-resin. In the proteomic analysis of the immunoprecipitates, shown in Table 1, ELMO was the most abundant protein detected in all MBC-HA runs aside from MBC itself. To further substantiate this interaction, reciprocal immunoprecipitations utilized embryos in which HA-tagged or untagged ELMO transgenes were expressed in the mesoderm under *mef2-GAL4* control. While the presence of MBC was not as apparent in total immunoprecipitated protein analyzed by silver staining, immunoblotting revealed a strong band that cross reacted with antisera against MBC. In samples analyzed by mass spectrometry, MBC was detected in all HA-ELMO immunoprecipitates, with spectral counts corresponding to the most abundant peptides detected after ELMO (Table 1). As anticipated from our previous studies, DCrk was not detected in samples of immunoprecipitated MBC or ELMO analyzed by MudPIT, nor were these proteins detected in samples of HA-tagged DCrk expressed in the embryonic musculature.

ELMO is expressed ubiquitously during oogenesis and embryogenesis

To examine the temporal expression pattern of *elmo* mRNA, RT-PCR was performed at various stages throughout *Drosophila* development (Fig. 2A). Much like *mbc*, the *elmo* transcript is abundant during oogenesis and provided maternally to the embryo, as evidenced by the presence of RT-PCR product in unfertilized eggs and embryos at 0–4 h AEL. Expression remains relatively high throughout embryogenesis, persists during the larval and pupal stages, and is detectable in the adult. The spatial expression pattern of ELMO, as revealed by antisera raised against the full length protein, is broad and cytoplasmic in the developing *Drosophila* ovary (Fig. 2B–C″). It is constant in the germline and becomes evident in the somatic follicle cells after stage 9 (Fig. 2B, arrow), with higher expression in the border cells (Fig. 2C inset, C ′, arrow) at stage 10. In the embryo, maternally-provided *elmo* transcript is high prior to stage 5, which coincides with the beginning of zygotic transcription (Fig. 2D). It is present in the developing mesoderm in stages 9–13 (Fig. 2E–G, arrows) and remains detectable in both the visceral and somatic musculature through Stage 16 (Fig. 2H, I, arrows). Staining with polyclonal rabbit antisera against ELMO reveals a broad temporal and spatial pattern of expression, consistent with the results of RT-PCR and in situ hybridization (data not shown).

Generation of EMS-induced mutations in *elmo*

Drosophila CG5336/ELMO has 47% overall similarity with *C. elegans* CED-12 and 45–54% with the three vertebrate ELMO proteins. All proteins contain the same signature domains (Fig. 3A). The primary amino acid sequence of the N terminal two thirds of ELMO shares no obvious homology with any protein domains. However, analysis of secondary structure using a homology detection/structure prediction program and psi-blast http://toolkit.tuebingen.mpg.de/hhpred) suggests that this region adopts a superhelical structure similar to that of the ARMADILLO/HEAT repeat, and includes five such repeats ((deBakker et al., 2004); Mushegian and Geisbrecht, unpublished). The PH domain is highly conserved, and all proteins contain a single proline-rich PxxP consensus sequence for binding to SH3 domains.

Genetic analysis of *elmo* was initiated using a lethal PiggyBac insertion in the first intron (*PB [c06760]*; Fig. 3B). The lethality of the insert is reverted by its excision or by expression of a

UAS-elmo transgene under control of *actin-GAL4.* Molecular analysis of embryos both maternally and zygotically mutant for *PB[c06760]* by RT-PCR revealed the presence of wild-type transcript as well as two larger products (Supp Fig. 1). The nucleotide sequence of these larger products indicates that the *PB[c06760]* insertion causes some aberrant splicing of the primary transcript between exons 1 and 2, and introduces a stop codon 8 amino acids downstream from the end of exon 1. Despite this perturbation, the presence of wild-type transcript suggests that *PB[c06760]* is a hypomorphic allele of *elmo*. To obtain null alleles, we carried out an F2 lethal screen of 5000 EMS-mutagenized chromosomes for individuals that failed to complement *PB[c06760]*. The molecular lesions of the resulting alleles are shown in Figure 3C and D. Stop codons have been introduced before the PH domain in $elmo^{19F3}$ and $elmo^{9F4}$, while $elmo^{8C6}$ represents a missense mutation in which a conserved glycine has been changed to arginine.

Reduced ELMO causes defects in border cell migration

Based on the observation that *mbc* has a role in border cell migration (Duchek et al., 2001), that ELMO is expressed in the border cells, and that ELMO interacts physically with MBC, we examined whether ELMO is also required for border cell migration. In this process, a group of 8–10 border cells are recruited from the anterior follicle cells during stage 9, and migrate between the nurse cells until they reach the nurse cell/oocyte border at stage 10 (Fig. 4A). To examine the requirement for *elmo* during this migration, expression of *UAS-elmo RNAi* was directed to the border cells using the *slbo-GAL4* driver. The RNAi-mediated reduction of *mbc* serves as a positive control and, as expected, results in severe defects in border cell migration in which approximately 40% of the stage 10 egg chambers contain cell clusters that fail to reach the nurse cell/oocyte border (Fig. 4B). Similar, but weaker, effects are caused by an RNAi-mediated reduction in *elmo*. Two independent transgenic lines, each expressing one copy of *UAS-elmo RNAi,* cause mild defects in which 20% of the border cells fail to migrate completely (Fig. 4B). The penetrance of this defect increases to 40% in the presence of two copies of *UAS-elmo RNAi*. Co-expression of *UAS-mbc RNAi* and *UAS-elmo RNAi* transgenes further increases the severity and penetrance of the defects, such that 55% of the border cells fail to migrate completely. By comparison, co-expression of *UAS-DCrk RNAi* and *UAS-mbc RNAi* increases the observed defects in border cell migration only slightly over those observed for each transgene alone. Similar results were obtained when the above transgenes were driven in the border cells using *c306-Gal4* driver (data not shown).

To ensure that the RNAi effects observed in border cell migration are due to a reduction in *elmo* gene function, mosaic clones of border cells lacking all *elmo* expression were generated using the $elmo^{19F3}$ stop codon allele. As described recently by others (Bianco et al., 2007), we observed severe migration defects in border cells lacking *elmo* with 35% showing no migration at all and the remaining 65% arresting their journey when only 25% complete (Fig. 4C–F′ and data not shown).

ELMO is required for myoblast fusion

Since the MBC SH3 domain is essential for embryonic myoblast fusion (Balagopalan et al., 2006) and this domain interacts with ELMO, we examined whether loss of *elmo* resulted in defects in myoblast fusion. Embryos homozygous for $elmo^{PB[c06760]}$ or $elmo^{8C6}$, both of which are hypomorphic alleles, have minor defects in which a small number of myoblasts remain unfused and muscles are occassionally missing (data not shown). Embryos trans-heterozygous for $elmo^{PB[c06760]}$ or $elmo^{8C6}$ and *Df(2L)HO55,* a deficiency that removes *elmo,* also exhibit very modest perturbations. The overall muscle pattern is unperturbed in these embryos, but some unfused myoblasts are present just under the muscle layer when compared to wild-type embryos in which these unfused myoblasts are not present (Fig. 5A, A′, C–D′). A larger number of unfused myoblasts as well as missing muscles are apparent in *Df(2L)HO55/Df(2L)HO55*

embryos (Fig. 5B, B′) and embryos trans-heterozygous for *Df(2L)HO55* and either *elmo*^{9F4} or *elmo*^{19F3}, the latter of which contain stop codons and are therefore likely to be protein null (Fig. 5E, F). Of note, the unfused myoblasts are most abundant and more easily visualized in the focal plane just below the muscle layer (Fig. 5E′, F′).

The presence of maternally provided transcript and the variable penetrance of the embryonic muscle defects suggested that the perdurance of maternal *elmo* mRNA and/or its protein product may be obscuring the loss of function muscle phenotype. To address this hypothesis, germline clones (GLCs) were generated to eliminate both maternal and zygotic *elmo* transcripts. GLCs of e*lmo*^{9F4} do not survive oogenesis, likely due to the presence of a lethal background mutation. GLC embryos mutant for *elmo*^{19F3} die prior to myogenesis, possibly reflecting an earlier embryonic requirement for *elmo*. We therefore examined GLC embryos maternally mutant for *elmo*$^{PB[c06760]}$ or *elmo*^{8C6} and zygotically heterozygous for *Df(2L) Prl*, which removes *elmo*, with the hope that these hypomorphic alleles would provide sufficient transcript for early embryogenesis, and allow later visualization of the musculature under conditions of reduced *elmo*. As shown in Figure 6A and B, these embryos exhibit a greater number of missing muscles and unfused myoblasts (Fig. 6A′, B′) compared to zygotic trans-heterozygotes of the hypomporphic alleles *elmo*$^{PB[c06760]}$ or *elmo*^{8C6}. Thus, both the maternal and zygotic transcripts contribute to ELMO's role in the embryonic musculature

Given the almost ubiquitous expression of elmo, and its requirement prior to myoblast fusion, we sought to determine whether the myoblast fusion defects observed in *elmo* mutants reflect an earlier role in muscle cell fate commitment. To address this possibility, we analyzed *elmo* maternal and zygotic mutants with various mesodermal markers. DMEF2 is expressed in all developing muscle cells and is required for their differentiation. Similar numbers of DMEF2 positive cells are observed in both WT and *elmo* mutant embryos (Fig. 6C, D), suggesting that a decrease in elmo does not impact their specification. Likewise, specification of founder cells and fusion competent cells appears to have occurred normally in elmo mutants, as visualized using antibodies against Kruppel (Kr) and Sticks and stones (SNS), respectively (Fig. 6E–H). To determine if the muscle defects observed in *elmo* mutants are autonomous to the muscle and not a result of secondary defects in other tissues, we expressed *UAS-elmoIR* in the muscle under the control of *mef2-GAL4*. Due to the presence of maternal load and the variability in which RNAi works in tissues, it is not surprising that gross defects in the final muscle pattern were not observed. However, an approximately two-fold increase in unfused myoblasts were observed in stage 16 embryos expressing two copies of *elmo* RNAi compared to *mef2-GAL4* control embryos at 29°C. Presumably due to higher temperatures which can result in minor developmental defects, control embryos showed an average of 26.8 unfused myoblasts (SD=9.7; n=11) in hemisegments A1–A5 as visualized by immunofluorescence with anti-MHC (data not shown). Embryos expressing *elmo* RNAi in the musculature showed an average of 49.3 unfused myoblasts/A1–A5 hemisegments with a SD=9.0 (n=9) with a confidence level of >99.0%. This data strongly suggests that the elmo-associated defects in myoblast fusion are autonomous to the musculature, and due to a block in fusion rather than a decrease in properly specified cells.

MBC and ELMO function in concert to disrupt myoblast fusion

Mesodermal expression of constitutively-active Rac1 has previously been shown to have a negative impact on muscle development, severely impairing myoblast fusion (Luo et al., 1994). Since MBC and ELMO are predicted to function together to activate Rac1, by analogy to their orthologs, it was of interest to determine whether excess MBC and ELMO collaborate to perturb myoblast fusion. The *mef2-GAL4* driver was used to direct expression of *UAS-mbc*, *UAS-elmo*, or both, to the developing musculature. Representative embryos from this analysis are shown in Figure 7, and demonstrate that neither an increase in MBC nor an increase

in ELMO cause obvious muscle perturbations (Fig. 7A–C). By contrast, an excess of both MBC and ELMO has a profound effect on myoblast fusion (Fig. 7D), indicating that they work together to induce downstream events. These data are consistent with the results of our mass spectrometry analysis, which demonstrate that MBC and ELMO interact stoichiometrically in the musculature, and suggest that this is the functional form of the two proteins.

MBC and ELMO function as a Rac-GEF in the developing eye

The *Drosophila* eye, where genetic interactions are easily observed, has been used extensively to study proteins required for GTPase signaling, including Rac1 and Rac2 (Hakeda-Suzuki et al., 2002; Nolan et al., 1998). Of note, *mbc* was identified as a suppressor of a rough eye phenotype induced by excess wild-type Rac1 (Nolan et al., 1998). To test the idea that MBC and ELMO act in concert to activate Rac *in vivo*, we analyzed genetic interactions in the eye. As in the embryonic muscle, neither excess MBC nor excess ELMO alone have an impact on ommatidial organization (Fig. 8A, B). However, coincident expression of MBC and ELMO causes a rough eye phenotype (Fig. 8C). The rough eye phenotype is suppressed by a reduction in endogenous mbc or elmo (Fig. 8E), confirming that these proteins function stoichiometrically and that the rough eye phenotype is not due to forced interactions with other proteins. More importantly, the rough eye phenotype appears to reflect activation of endogenous Rac proteins by the MBC/ELMO complex, since it is sensitive to the dosage of these GTPases (Fig. 8D).

As a final confirmation that MBC and ELMO act together to recapitulate Rac-GEF activity, we performed an analysis similar to that described by Huelsmann (Huelsmann et al., 2006). We took advantage of the severe rough eye phenotype caused by expression of RacN17, which is characterized by fused ommatidia and missing bristles ((Fan and M., 1994); Fig. 8F, Supp. Fig. 2). This dominant-negative form of Rac is thought to sequester free GEFs in the cell. Thus an increase in the MBC/ELMO complex would provide additional GEF to activate Rac, thereby suppressing the eye perturbations cased by RacN17. Indeed, co-expression of MBC and ELMO suppresses the rough eye phenotype caused by RacN17 (Fig. 8G, Supp. Fig. 2), indicating that these proteins function together as a Rac-GEF.

DISCUSSION

The CDM signaling pathway in *Drosophila* includes the DOCK180/CED-5 ortholog MBC. Like conventional GEFs, DOCK180 and CED-5 contain highly conserved domains that can bind to monomeric GTPases and contribute to their activation (Meller et al., 2005). However, the conserved PH-domain that is normally present within conventional GEFs is actually provided by a separate protein family represented by ELMO/CED-12 (Brugnera et al., 2002; Lu et al., 2004).. Thus, one member of each of these two protein families can combine to form an unconventional bipartite GEF. While the small adaptor protein Crk often forms a critical component of this complex, recent studies have suggested that both DOCK180 and MBC can function in its absence (Balagopalan et al., 2006; Tosello-Trampont et al., 2007). Moreover, Crk has been shown to function in pathways that are totally independent of this bipartite GEF (Sasahara et al., 2002; Tang et al., 2005). Reminscent of this diversity of interactions, recent studies have suggested that CDM and ELMO/CED-12 family proteins may also function through independent interactions. For example, DOCK180 is capable of activating Rac on its own and has positive effects on cell migration and phagocytosis, albeit enhanced by binding of ELMO (Brugnera et al., 2002; Katoh and Negishi, 2003; Lu et al., 2004), and ELMO interacts with radizin independent of its interaction with DOCK180 (Grimsley et al., 2005). *Drosophila* MBC functions in a wide variety of processes that include border cell migration in the ovary and myoblast fusion in the embryo (Duchek et al., 2001; Erickson et al., 1997) and can contribute to the activation of Rac1 in the eye (Nolan et al., 1998). We have

demonstrated herein, through its biochemical and genetic analysis, that *Drosophila elmo* functions in concert with MBC in these processes. Like MBC, decreased levels of ELMO impair border cell migration and myoblast fusion ((Bianco et al., 2007) and studies herein). Moreover, MBC interacts stoichimetrically in the mesoderm with ELMO. Coincident over-expression of this complex impairs myoblast fusion, reinforcing the model from constitutively-active Rac1 that excess active Rac1 also interfers with myoblast fusion. Co-expression of MBC and ELMO also impacts development of the adult eye, resulting in a rough eye phenotype that is suppressed by decreasing endogenous levels of Rac. These data indicate that MBC and ELMO function together in a complex, and as a RacGEF.

ELMO is expressed and acts in concert with MBC during various stages in *Drosophila* development

As discussed above, CDM family proteins are required for a diverse array of biological processes. If ELMO functions with MBC in these processes, one would expect it to be expressed in a temporal and spatial pattern coincident with that of MBC. Consistent with this expectation, RT-PCR throughout the fly life cycle, embryonic *in situ* hybridizations and antibody stainings at multiple stages of *Drosophila* development, reveal that *elmo* is broadly expressed. Interestingly, however, the MBC/ELMO complex may serve distinct roles in each of the tissues in which it is expressed. MBC and ELMO are required for migration of the border cells in the ovary (Bianco et al., 2007; Duchek et al., 2001); however, myoblast migration appears to occur normally in *mbc* mutant embryos, as the fusion competent cells in *mbc* mutants can be found clustered and aligned with the founder cells

The CDM/ELMO(Ced-12) complexes in both vertebrate and *C. elegans* function upstream of Rac as unconventional bipartite GEFs to promote exchange of GDP for GTP in activation of monomeric GTPases (Meller et al., 2005). Our studies support a similar role for Drosophila MBC/ELMO. First, during ommatidial development, the rough eye phenotype resulting from co-expression of MBC and ELMO can be suppressed by removing half the gene dosage contributed by Rac1 and Rac2. Also, overexpression of the MBC/ELMO complex is sufficient to provide enough GEF activity to overcome the effect of its sequestration by RacN17 in the eye. In both the musculature and eye, expression of neither MBC nor ELMO alone has a phenotypic consequence, yet co-expression of MBC and ELMO phenocopies activated Rac.

Noteably, embryos that are completely lacking both maternal and zygotic *elmo* die before muscle development occurs, possibly reflecting an earlier role for the protein. Interestingly, however, the development of mutant embryos that lack both maternally and zygotically provided *mbc* continues until myogenesis (Balagopalan et al., 2006). These data suggest that, like its vertebrate counterparts, *Drosophila* ELMO has multiple binding partners. In addition to DOCK180, vertebrate ELMOs bind to three of the five additional CDM family members, suggesting that ELMO binding is a general feature of these proteins (Grimsley et al., 2004; Sanui et al., 2003). Based upon primary sequence homology, the fly genome contains at least four potential CDM superfamily members in addition to MBC (Cote and Vuori, 2002) The predicted transcripts of two of these are most closely related to vertebrate DOCK9/11 and DOCK 7/8. The *Drosophila* protein most closely related to vertebrate DOCK4 has been reported as the protein product of the *sponge* locus (Postner et al., 1992), but has not been studied extensively. It remains to be seen whether *Drosophila* ELMO is capable of binding to these other CDM-like molecules, and functions in concert with them in other tissues. One such place to examine in this regard is the embryonic CNS, where ELMO expression is quite strong but MBC is strikingly low (Erickson et al., 1997). Thus, alternative CDM/ELMO-like complexes may be present and required in different tissues throughout *Drosophila* development, or in the same tissues to regulate different GTPases.

Interaction of ELMO with other proteins and CDM/ELMO integration with other signaling pathways

The above studies, combined with recent reports of ELMO binding to non-CDM family members, may reflect a role for ELMO proteins in integrating signals from different pathways. Interaction of the N-terminal region of ELMO with RhoG is capable of translocating the ELMO/DOCK180 complex to the membrane to regulate neurite outgrowth and cell migration (Katoh and Negishi, 2003). Simultaneously, the N-terminal region of ELMO can bind to both the inactive and active forms of the ERM protein radixin (Grimsley et al., 2005). Interestingly, this ELMO/radixin interaction does not affect the ability of the ELMO/DOCK180 complex to promote Rac activation (Grimsley et al., 2005). Hence, ELMO may be functioning at the membrane to regulate the actin cytoskeleton via Rac, while recruiting radixin and ERM family members to perform their recognized roles in cross-linking the actin cytoskeleton to the plasma membrane.

In addition to Rac activation via the CDM/ELMO proteins, the ARF (ADP-ribosylaton factor) family of GTPases has been shown to signal through Rac (D'Souza-Schorey and Chavrier, 2006). Both DOCK180 and ELMO colocalize with ARNO (an ARF-GEF) and overexpression of mutant forms of DOCK180 and ELMO mutants block ARNO-induced Rac activation (Santy et al., 2005). However, RhoG signaling does not seem to be required for the ARNO-ELMO activation of Rac (Santy et al., 2005). This suggests Rac activation is differentially regulated in cell or tissue-specific manners or that within a cell there are localized mechanisms defined by crosstalk between signaling pathways that are responsible for Rac membrane localization. Intriguingly, in the *Drosophila* musculature, expression of a dominant-negative ARF6 results in myoblast fusion defects while the corresponding ARF-GEF Loner/Schizo is required for membrane localization of Rac (Chen et al., 2003). More work is required to see if ARF6, Loner/Schizo, and the ELMO/MBC proteins function in a signaling pathway in *Drosophila* to activate Rac.

Rac activity and myoblast fusion

Numerous studies have established a crucial role for Rac activation in myoblast fusion. More than a decade ago, Luo and colleagues demonstrated that a dominant-negative form of Rac1 interferes with myoblast fusion (Luo et al., 1994). A herculean genetic analysis of the small Rac GTPases proved that the fusion defects observed with dominant-negative Rac1 reflect the *Rac1, Rac2* loss-of-function phenotype (Hakeda-Suzuki et al., 2002) The need for activated Rac in myoblast fusion was further supported by the phenotype of embryos mutant for *mbc* (Erickson et al., 1997) and *elmo*, as shown herein. Rac, in turn, likely functions to direct rearrgangement of the actin cytoskeleton through regulation of the Arp2/3 complex via Kette and WAVE (Chen and Olson, 2005). Surprisingly, however, constitutively-active forms of Rac negatively impact this process in a manner that, on the surface, have the same phenotypic consequence as the absence of active Rac (Luo et al., 1994). The specific relevance of excess activated Rac1 to normal myoblast fusion remains unclear, and we cannot rule out that excess Rac interferes with other signaling pathways that do not normally impact myoblast fusion. However, perturbation of this phenotype also has the potential to uncover key components and regulators that contribute to the normal process.

Our data establish, for example, that monomeric Rac GTPases are in excess, and are therefore available to be activated when the level of the MBC/ELMO GEF complex is increased. Under normal circumstances, then, the ability of the cell to activate this endogenous Rac remains low. Potential mechanisms for this include the direct regulation of MBC and/or ELMO levels through synthesis or turnover. Though little is known about the synthesis of either MBC or ELMO or their levels in the cell, it is intriguing that DOCK180 is ubiquitinated and this modification ensures its rapid turnover (Makino et al., 2006). Alternatively, GAPs may be

present to ensure that Rac does not remain active. Finally, the MBC/ELMO pathway may be integrating with the loner-Arf6 associated pathway, as discussed above, in such a way that perturbation of MBC and ELMO is impacting Rac1 activity through components of the Arf6 pathway. Either way, the fact that this myoblast fusion phenotype is occurring in response to perturbation of the endogenous pathway by wild-type proteins in a stoichiometric manner suggests that it may be possible to modulate it in ways that provide insights into the myoblast fusion process.

Supplementary Material

Refer to Web version on PubMed Central for supplementary material.

Acknowledgments

We thank Jeff Haug and Josh Wunderlich of the Stowers Institute Cytometry and Molecular Biology Core Facilities for assistance. We thank members of the Abmayr lab, particularly Claude Shelton, Kiran Kocherlakota, David Ash and Maggie Chen for helpful discussions and assistance. ERG was supported by a Ruth Kirschstein NRSA fellowship; Grant Number F32A053027 from the National Institute of Arthritis and Musculoskeletal And Skin Diseases. This work was supported by the Stowers Institute for Medical Research and NIH grant RO1 AR44274 to S.M. Abmayr.

References

Balagopalan L, et al. The CDM superfamily protein MBC directs myoblast fusion through a mechanism that requires phosphatidylinositol 3,4,5-triphosphate binding but is independent of direct interaction with DCrk. Mol Cell Biol 2006;26:9442–55. [PubMed: 17030600]

Bianco A, et al. Two distinct modes of guidance signalling during collective migration of border cells. Nature 2007;448:362–5. [PubMed: 17637670]

Bourne HR. Rac and cell migration: CDM proteins integrate signals. Nat Cell Biol 2005;7:777–8. [PubMed: 16056271]

Brugnera E, et al. Unconventional Rac-GEF activity is mediated through the Dock180-ELMO complex. Nat Cell Biol 2002;4:574–82. [PubMed: 12134158]

Chang HY, Ready DF. Rescue of photoreceptor degeneration in rhodopsin-null Drosophila mutants by activated Rac1. Science 2000;290:1978–80. [PubMed: 11110667]

Chen EH, Olson EN. Antisocial, an intracellular adaptor protein, is required for myoblast fusion in Drosophila. Dev Cell 2001;1:705–15. [PubMed: 11709190]

Chen EH, Olson EN. Unveiling the mechanisms of cell-cell fusion. Science 2005;308:369–73. [PubMed: 15831748]

Chen EH, et al. Control of myoblast fusion by a guanine nucleotide exchange factor, loner, and its effector ARF6. Cell 2003;114:751–62. [PubMed: 14505574]

Cheresh DA, et al. Regulation of Cell Contraction and Membrane Ruffling by Distinct Signals in Migratory Cells. The Journal of Cell Biology 1999;146:1107–1116. [PubMed: 10477763]

Cote JF, et al. A novel and evolutionarily conserved PtdIns(3,4,5)P(3)-binding domain is necessary for DOCK180 signalling. Nat Cell Biol 2005;7:797–807. [PubMed: 16025104]

Cote JF, Vuori K. Identification of an evolutionarily conserved superfamily of DOCK180-related proteins with guanine nucleotide exchange activity. J Cell Sci 2002;115:4901–13. [PubMed: 12432077]

D'Souza-Schorey C, Chavrier P. ARF proteins: roles in membrane traffic and beyond. Nat Rev Mol Cell Biol 2006;7:347–58. [PubMed: 16633337]

de Bakker CD, et al. Phagocytosis of apoptotic cells is regulated by a UNC-73/TRIO-MIG-2/RhoG signaling module and armadillo repeats of CED-12/ELMO. Curr Biol 2004;14:2208–16. [PubMed: 15620647]

Duchek P, et al. Guidance of cell migration by the Drosophila PDGF/VEGF receptor. Cell 2001;107:17–26. [PubMed: 11595182]

Eng JK, et al. An approach to correlate tandem mass spectral data of peptides with amino acid sequences in a protein database. J Am Soc Mass Spectrom 1994;5:976–989.

Erickson MRS, et al. *Drosophila myoblast city* encodes a conserved protein that is essential for myoblast fusion, dorsal closure and cytoskeletal organization. Journal of Cell Biology 1997;138:589–603. [PubMed: 9245788]

Fan C-MMT-L. Patterning of mammalian somites by surface ectoderm and notochord: evidence for schlerotome induction by a hedgehog homolog. Cell 1994;79:1175–1186. [PubMed: 8001153]

Florens L, Washburn MP. Proteomic analysis by multidimensional protein identification technology. Methods Mol Biol 2006;328:159–75. [PubMed: 16785648]

Geisbrecht ER, Montell DJ. A role for Drosophila IAP1-mediated caspase inhibition in Rac-dependent cell migration. Cell 2004;118:111–25. [PubMed: 15242648]

Grimsley CM, et al. Dock180 and ELMO1 proteins cooperate to promote evolutionarily conserved Rac-dependent cell migration. J Biol Chem 2004;279:6087–97. [PubMed: 14638695]

Grimsley CM, et al. Characterization of a novel interaction between ELMO1 and ERM proteins. J Biol Chem 2005;291:5928–5937. [PubMed: 16377631]

Gumienny TL, et al. CED-12/ELMO, a novel member of the CrkII/Dock180/Rac pathway, is required for phagocytosis and cell migration. Cell 2001;107:27–41. [PubMed: 11595183]

Hakeda-Suzuki S, et al. Rac function and regulation during Drosophila development. Nature 2002;416:438–42. [PubMed: 11919634]

Hasegawa H, et al. DOCK180, a major CRK-binding protein, alters cell morphology upon translocation to the cell membrane. Molecular and Cellular Biology 1996;16:1770–1776. [PubMed: 8657152]

Huelsmann S, et al. The PDZ-GEF dizzy regulates cell shape of migrating macrophages via Rap1 and integrins in the Drosophila embryo. Development 2006;133:2915–24. [PubMed: 16818452]

Ishimaru S, et al. PVR plays a critical role via JNK activation in thorax closure during Drosophila metamorphosis. Embo J 2004;23:3984–94. [PubMed: 15457211]

Katoh H, Negishi M. RhoG activates Rac1 by direct interaction with the Dock180-binding protein Elmo. Nature 2003;424:461–4. [PubMed: 12879077]

Kinchen JM, et al. Two pathways converge at CED-10 to mediate actin rearrangement and corpse removal in C. elegans. Nature 2005;434:93–9. [PubMed: 15744306]

Kiyokawa E, et al. Evidence that DOCK180 up-regulates signals from the CrkII-p130(Cas) complex. J Biol Chem 1998;273:24479–84. [PubMed: 9733740]

Kobayashi S, et al. Membrane recruitment of DOCK180 by binding to PtdIns(3,4,5)P3. Biochem J 2001;354:73–8. [PubMed: 11171081]

Lu M, et al. PH domain of ELMO functions in trans to regulate Rac activation via Dock180. Nat Struct Mol Biol 2004;11:756–62. [PubMed: 15247908]

Lu M, et al. A Steric-inhibition model for regulation of nucleotide exchange via the Dock180 family of GEFs. Curr Biol 2005;15:371–7. [PubMed: 15723800]

Luo L, et al. Distinct morphogenetic functions of similar small GTPases: Drosophila Drac1 is involved in axonal outgrowth and myoblast fusion. Genes Dev 1994;8:1787–802. [PubMed: 7958857]

Makino Y, et al. Elmo1 inhibits ubiquitylation of Dock180. J Cell Sci 2006;119:923–32. [PubMed: 16495483]

McDonald WH, et al. Comparison of three directly coupled HPLC MS/MS strategies for identification of proteins from complex mixtures: single-dimension LCMS/MS, 2-phase MudPIT, and 3-phase MudPIT. Int J Mass Spectrom 2002;219:245–251.

Meller N, et al. CZH proteins: a new family of Rho-GEFs. J Cell Sci 2005;118:4937–46. [PubMed: 16254241]

Niewiadomska P, et al. DE-Cadherin is required for intercellular motility during Drosophila oogenesis. J Cell Biol 1999;144:533–47. [PubMed: 9971747]

Nolan KM, et al. Myoblast city, the Drosophila homolog of DOCK180/CED-5, is required in a Rac signaling pathway utilized for multiple developmental processes. Genes Dev 1998;12:3337–42. [PubMed: 9808621]

Paoletti AC, et al. Quantitative proteomic analysis of distinct mammalian Mediator complexes using normalized spectral abundance factors. Proc Natl Acad Sci U S A 2006;103:18928–33. [PubMed: 17138671]

Postner MA, et al. Maternal effect mutations of the sponge locus affect actin cytoskeletal rearrangements in Drosophila melanogaster embryos. J Cell Biol 1992;119:1205–18. [PubMed: 1447298]

Reif K, Cyster J. The CDM protein DOCK2 in lymphocyte migration. Trends Cell Biol 2002;12:368–73. [PubMed: 12191913]

Santy LC, et al. The DOCK180/Elmo complex couples ARNO-mediated Arf6 activation to the downstream activation of Rac1. Curr Biol 2005;15:1749–54. [PubMed: 16213822]

Sanui T, et al. DOCK2 regulates Rac activation and cytoskeletal reorganization through interaction with ELMO1. Blood 2003;102:2948–50. [PubMed: 12829596]

Sasahara Y, et al. Mechanism of recruitment of WASP to the immunological synapse and of its activation following TCR ligation. Mol Cell 2002;10:1269–81. [PubMed: 12504004]

Tabb DL, et al. DTASelect and Contrast: tools for assembling and comparing protein identifications from shotgun proteomics. J Proteome Res 2002;1:21–6. [PubMed: 12643522]

Tang DD, et al. The adapter protein CrkII regulates neuronal Wiskott-Aldrich syndrome protein, actin polymerization, and tension development during contractile stimulation of smooth muscle. J Biol Chem 2005;280:23380–9. [PubMed: 15834156]

Tautz D, Pfeifle C. A non-radioactive *in situ* hybridization method for the localization of specific RNAs in *Drosophila* embryos reveals translational control of the segmentation gene hunchback. Chromosoma 1989;98:81–85. [PubMed: 2476281]

Tosello-Trampont AC, et al. Identification of two signaling submodules within the CrkII/ELMO/Dock180 pathway regulating engulfment of apoptotic cells. Cell Death Differ 2007;14:963–72. [PubMed: 17304244]

Washburn MP, et al. Large-scale analysis of the yeast proteome by multidimensional protein identification technology. Nat Biotechnol 2001;19:242–7. [PubMed: 11231557]

Wu YC, Horvitz HR. The C. elegans cell corpse engulfment gene ced-7 encodes a protein similar to ABC transporters. Cell 1998a;93:951–60. [PubMed: 9635425]

Wu YC, Horvitz HR. C. elegans phagocytosis and cell-migration protein CED-5 is similar to human DOCK180. Nature 1998b;392:501–4. [PubMed: 9548255]

Wu YC, et al. C. elegans CED-12 acts in the conserved crkII/DOCK180/Rac pathway to control cell migration and cell corpse engulfment. Dev Cell 2001;1:491–502. [PubMed: 11703940]

Zhou Z, et al. The C. elegans PH domain protein CED-12 regulates cytoskeletal reorganization via a Rho/Rac GTPase signaling pathway. Dev Cell 2001;1:477–89. [PubMed: 11703939]

Zybailov B, et al. Statistical analysis of membrane proteome expression changes in Saccharomyces cerevisiae. J Proteome Res 2006;5:2339–47. [PubMed: 16944946]

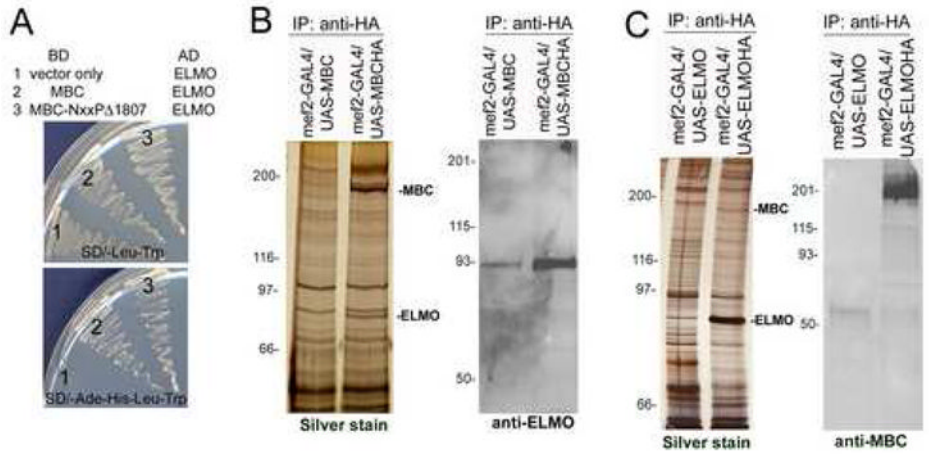

Figure 1.

Identification of ELMO as a binding partner for MBC. (A) Yeast two-hybrid assay. Growth on selective media is shown on the lower panel where both full-length and truncated MBC exhibit interaction with ELMO. (B, C) Anti-HA immunoprecipitates from lysates of untagged and HA-tagged MBC (B) and ELMO (C) expressed in the *Drosophila* mesoderm under control of *mef2-GAL4*. (B) The silver stained gel (left panel) shows a band of ~83kD that co-precipitates with MBC-HA. This band is revealed as ELMO by mass spectrometry and Western blotting with an antisera against ELMO (right panel). (C) The silver stained gel (left panel) shows a band of ~200kD that co-precipitates with ELMO-HA. This band is identified as MBC by mass spectrometry and Western blotting with an antisera against MBC (right panel).

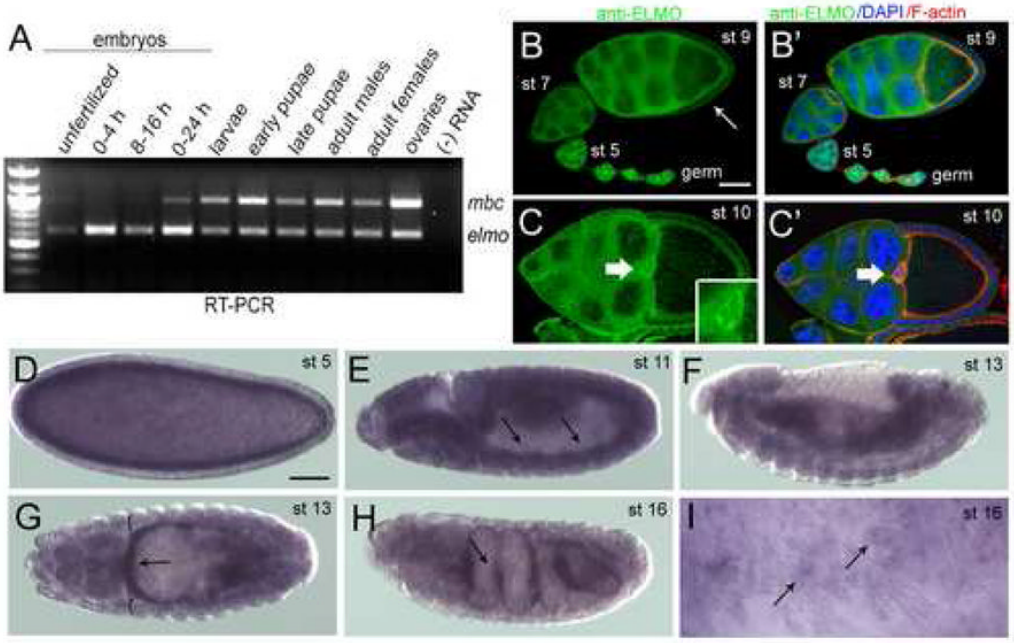

Figure 2.

Temporal and spatial expression patterns of *elmo*. (A) Temporal expression of *mbc* and *elmo* transcript by RT-PCR at specific developmental stages in the *Drosophila* life cycle (B–C′) Immunoreactivity of ELMO antisera in wild-type ovarioles. (B) ELMO is high in the germline at all stages of ovariole development, and is detected in the somatic follicle cells around stage 9 (arrow). (B′) DAPI (blue) and F-actin (red) do not extensively overlap with ELMO (green). (C) ELMO expression is ubiquitous in both the germline and somatic follicle cells of a stage 10 egg chamber, and is especially prominent in the border cells (arrow, inset). (C′) DAPI (blue) and F-actin (red) do not overlap extensively with ELMO (green). (D–I) *in situ* analysis of *elmo* in wild-type embryos. (D) *elmo* is detected at stage 5, suggesting that it is provided maternally. (E) Expression is fairly ubiquitous throughout the embryo, with mesodermal expression (arrows) becoming apparent by stage 11. (F, G) Stage 13 embryo in which expression is broad, but stronger in the gut visceral mesoderm (arrows) than in the somatic mesoderm (brackets). (H) Expression is highest (arrow) in the visceral mesoderm at stage 16. (I) High magnification view of the somatic mesoderm showing *elmo* expression in the mature muscle. Lateral views are shown in (D–F, H–I) and a dorsal view in G. Scale bar, 50μM

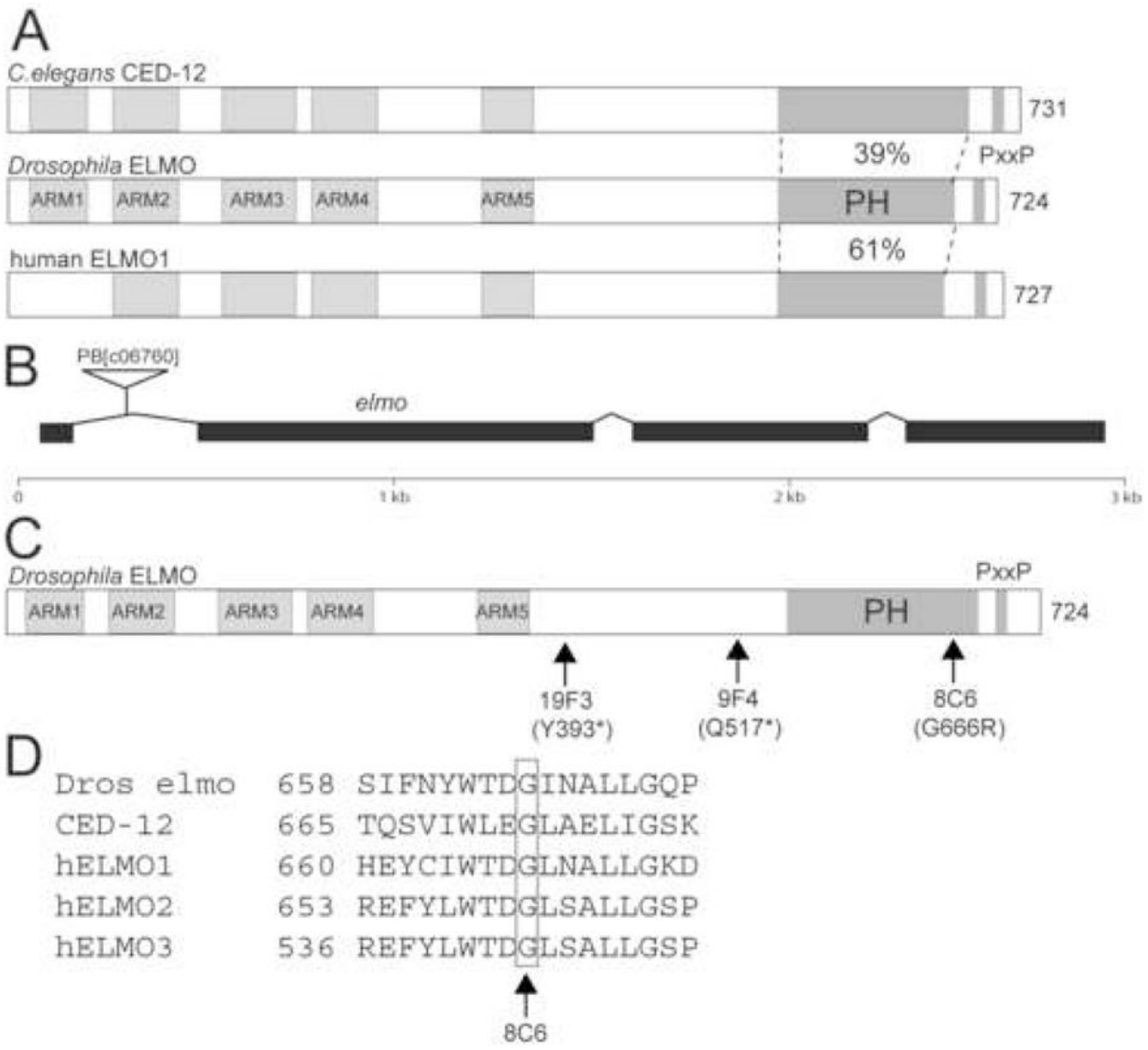

Figure 3.

CG5336 encodes ELMO/Dced-12. (A) *Drosophila* ELMO is the ortholog of *C. elegans* CED-12 and human ELMO1. The N-termini of these proteins share predicted Armadillo repeats, while the C-terminal region contains a pleckstrin homology (PH) domain and proline-rich region. (B) The intron/exon organization of the *CG5336/elmo* locus is shown. The PiggyBac transposable element *PB[c06760]* is located in the first intron. (C) The molecular lesions obtained in an EMS screen for *elmo* mutants are indicated. (D) The molecular lesion in the EMS-induced allele $elmo^{8C6}$ occurs in a conserved glycine at amino acid position 666 within the PH domain.

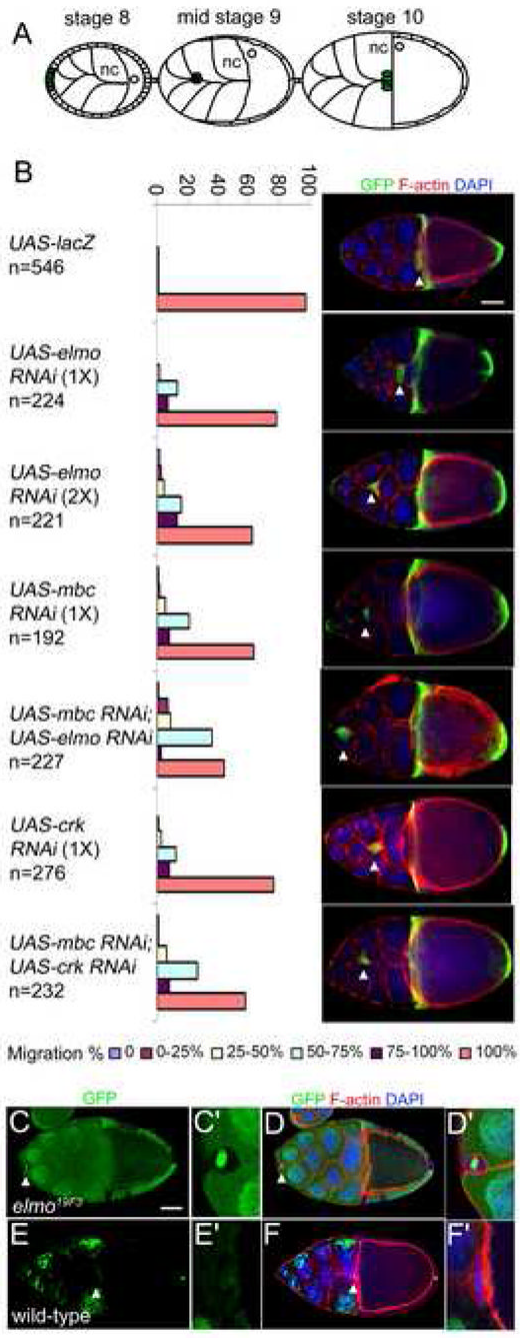

Figure 4.

Abrogation of *elmo* function results in border cell migration defects.

(A) Schematic of egg chambers at stages 8–10. Nurse cells (nc), oocyte (o) and border cells (green) are indicated. (B) Quantification of border cell migration defects in stage 10 egg chambers expressing the indicated RNAi transgene. Transgene expression is driven by *slbo-Gal4*, in a genetic background that also includes *UAS-mCD8-GFP*. The number of stage 10 egg chambers examined for each genotype is provided. A confocal image of one representative stage10 egg chamber is provided for each genotype to show the migration defect. The arrowhead in each indicates the position of the border cells. Egg chambers were stained for GFP (green), F-actin (phalloidin, red) and DAPI (blue). (C–F′) Mosaic analysis of $elmo^{19F3}$.

Confocal images of stage 10 egg chambers of *elmo*^{19F3} (C–D) and wild-type (E–F). High magnification views of the same border cell cluster which in the *elmo*^{19F3} mutant contain a mixture of GFP (green) positive and GFP negative cells and show no migration (C′) and in wild-type are all GFP negative and show complete migration (E′). (D–D′ and F–F′) Overlap with DAPI (blue) and F-actin (phalloidin, red) do not extensively overlap with GFP (green) expression. Arrowhead indicates the position of the border cells. Scale bar, 50μM

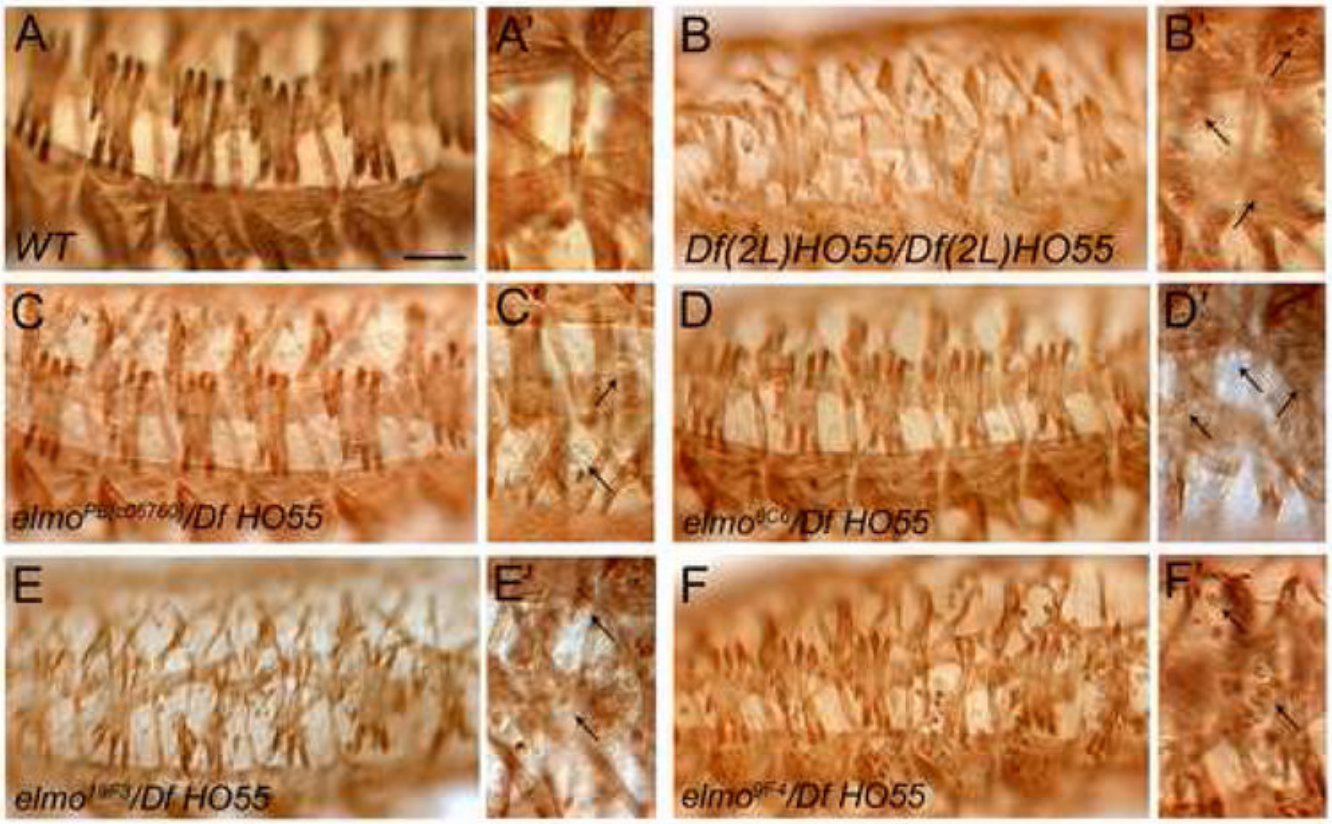

Figure 5.

Somatic muscle phenotype of *elmo* zygotic mutant embryos. (A–F′) Low and high magnification views of stage 16 embryos stained immunohistochemically with anti-MHC to reveal the muscle pattern. (A) Wild-type embryos showing the mature muscle pattern and lack of unfused myoblasts (A′). (B) Embryos homozygous mutant for *Df(2L)HO55*, a deficiency that removes *elmo*, exhibit missing muscles and unfused myoblasts (B′). (C, D) The muscle pattern appears to be unperturbed in transheterozygous embryos zygotically mutant for $elmo^{PB[c06760]}/Df\ HO55$ (C) and $elmo^{8C6}/Df\ HO55$ (D), with a few unfused myoblasts visible under the muscle layer (C′, D′, arrows). (E, F) Muscle fibers are missing in transheterozygous embryos zygotically mutant for $elmo^{19F3}/Df\ HO55$ (E) and $elmo^{9F4}/Df\ HO55$ (F), and many unfused myoblasts are apparent (E′, F′, arrows). Scale bar, 50μM

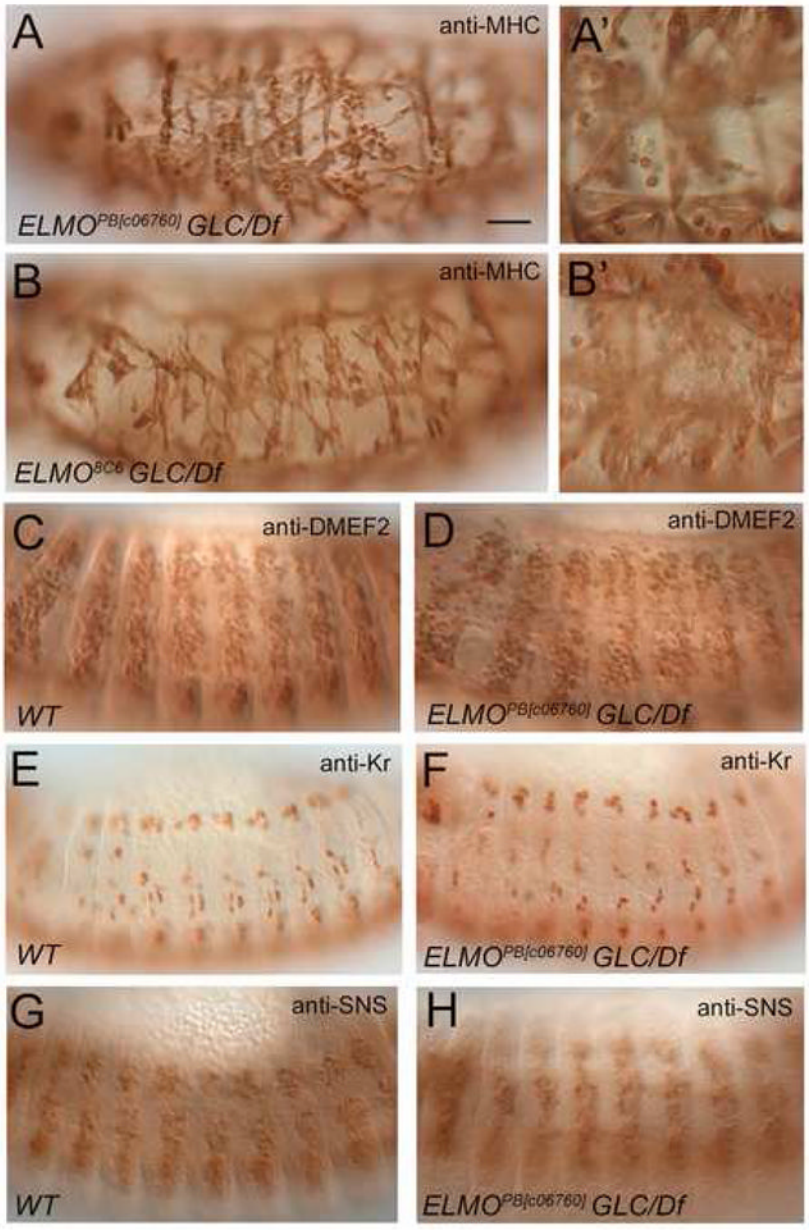

Figure 6.

Somatic muscle phenotype and muscle cell specification of maternal/zygotic *elmo* mutant embryos. (A-B′) Embryos from GLCs of $elmo^{PB[c06760]}$ or $elmo^{8C6}$, that are zygotically $elmo^{PB[c06760]}/Df(2R)Prl$ (A) or $elmo^{8C6}/Df(2R)Prl$ (B) exhibit a dramatic loss of muscles and increase in unfused myoblasts (A′, B′, arrows). (C-H) Wild-type and $elmo^{PB[c06760]}/Df(2R)Prl$ maternal/zygotic mutant embryos stained with anti-MEF2 (C, D) anti-Krüppel (Kr) (E, F), and anti-SNS (G, H) antibodies. (C,D) Similar number of MEF2-expressing cells are present in stage 14 wild-type and *elmo* mutants. (E, F) Stage 13 wild-type and *elmo* mutants exhibit founder cell positive cells as stained with the founder cell antibody Kr. (G, H) Similar staining patterns are observed with SNS antibody showing fusion competent cell fate is preserved in stage 13 wild-type and *elmo* mutants. All views are lateral, with anterior to the left and dorsal to the top. Scale bar, 50μM

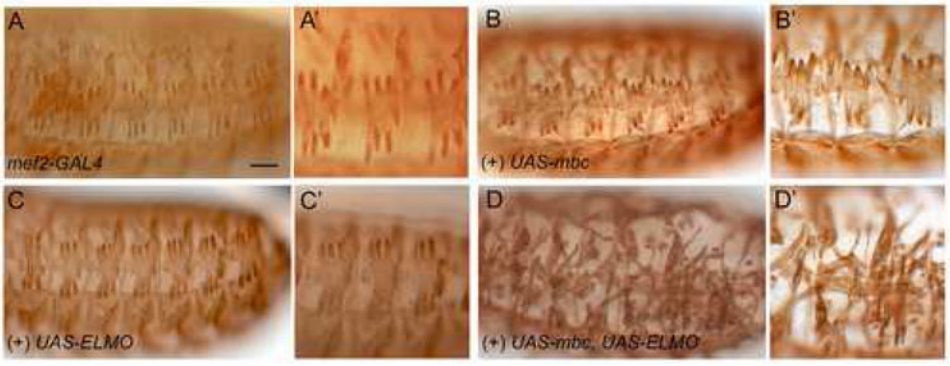

Figure 7.

Overexpression analysis of CDM pathway members in the musculature. (A–D′) Low magnification (A, B, C, D) and high magnification (A′ B′, C′, D′) views of stage 16 embryos expressing *UAS-cDNAs* under control of the pan-mesodermal *mef2*-GAL4 driver. (A, A′) Embryos of the genotype *mef2-GAL4* show a mature muscle pattern with no missing muscles and unfused myoblasts. (B–C′) Expression of *UAS-mbc* or *UAS-elmo*, respectively, has no effect on the muscle pattern. (D, D′) Co-expression of *UAS-elmo* and *UAS-mbc* results in missing muscles and many unfused myoblasts. All views are lateral, with anterior to the left and dorsal to the top. Scale bar, 50μM

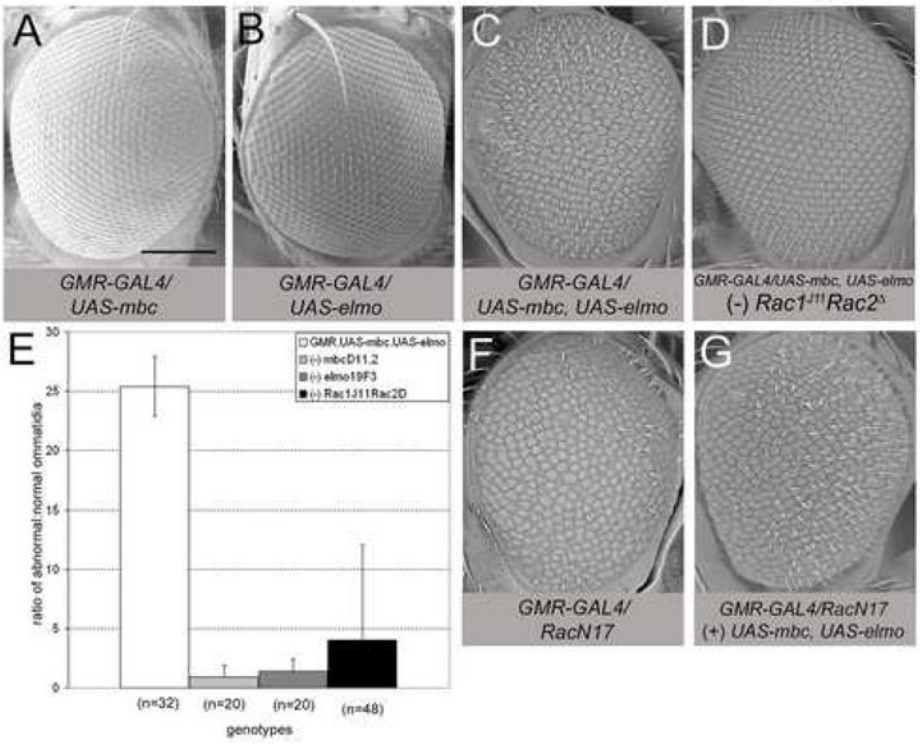

Figure 8.

Genetic interactions between *mbc*, *elmo*, and *Rac* alleles. (A–D, F, G) Scanning electron micrographs of adult eyes expressing *UAS-cDNAs* under control of *GMR-GAL4*. (A, B) Overexpression of *mbc* or *elmo* has no apparent impact on eye morphology. (C) Co-expression of *mbc* and *elmo* results in a severe rough eye phenotype. (D) Removal of one copy of $Rac1^{J11}Rac2^{\Delta}$ suppresses the rough eye phenotype, resulting in nearly wild-type eye morphology. (E) Graph depicting the ratio of abnormal:normal (A:N) ommatidia present in flies co-expressing *mbc* and *elmo* compared to flies co-expressing *mbc* and *elmo* in a heterozygous background for *mbc*, *elmo*, or *Rac1Rac2*. Adult eyes co-expressing *mbc* and *elmo* (white bar) exhibit a ratio of 25:1 (n=32) while the ratio of abnormal:normal ommatidia decreases when heterozygous for $mbc^{D11.2}$ (A:N=0.65; n=20), $elmo^{19F3}$ (A:N=0.51; n=20) or $Rac1^{J11}Rac2^{\Delta}$ (A:N=1.32; n=48). n is the number of eyes examined for each genotype. See also Supp Fig. 2(F, G) Expression of RacN17 results in a severe rough eye morphology (F) that is suppressed by coincident expression of *mbc* and *elmo* (G). Scale bar, 200μM

Table 1

Identification of Interacting proteins by MudPIT Analysis

MBC-interacting Proteins									
Protein	**Ti_1**	**Ti_2**	**Ti_3**	**Ti_4**	**Ti_5**	**Ti_6**	**Es_1**	**EC_1**	**Merged controls**
MBC	27.7%[a](164)[b]	4.4% (6)	28.8% (202)	49.2% (448)	5.3% (10)	11.6% (30)	11.2% (18)	6.2% (16)	1.7% (2)
CED-12	26.9% (61)	5.4% (4)	33.0% (84)	45.3% (131)	1.8% (1)	11.3% (9)	2.1% (1)	0.0% (1)	0.0% (0)
CRK	0.0% (0)	0.0% (0)	0.0% (0)	0.0% (0)	0.0% (0)	0.0% (0)	0.0% (0)	0.0% (0)	0.0% (0)
CED-12 interacting Proteins									
Protein	Ti_1	Ti_2	Ti_3	Ti_4	Ti_5	Es_1	Es_2	Es_3	Merged controls
CED-12	42.5%[a](2043)[b]	69.7% (1151)	74.5% (1985)	50.1% (2923)	70.7% (2923)	71.1% (867)	73.8% (790)	65.5% (432)	1.8% (2)
MBC	7.2% (89)	27.4% (118)	39.3% (244)	27.9% (398)	31.3% (245)	25.4% (112)	8.4% (18)	2.3% (5)	0.0% (0)
CRK	0.0% (0)	0.0% (0)	0.0% (0)	0.0% (0)	0.0% (0)	0.0% (0)	0.0% (0)	0.0% (0)	0.0% (0)

[a] Sequence coverage, percentage of the protein sequence covered by detected peptides identified by tandem mass spectroscopy

[b] Spectral counts, total spectra matching peptides detected by tandem mass spectroscopy

Ti=trypsin

Es=elastase

EC=endoproteinase Glu-C